ENHANCED KNOWLEDGE IN SCIENCES AND TECHNOLOGY
e-ISSN: 2773-6385

EKST

Vol. 6 No. 1 (2026) 698-708
https://publisher.uthm.edu.my/periodicals/index.php/ekst

Characterization of Nickel Thin Films as Strain Sensors for Wearable Health Monitoring System

Nur Khairunnisa Amrang[1], Ahmad Hadi Ali[1]*

[1] *Department of Physics and Chemistry, Faculty of Applied Sciences and Technology, UTHM Kampus Cawangan Pagoh, Hab Pendidikan Tinggi Pagoh, KM 1, Jalan Panchor, 84600 Pagoh, Muar, Johor, MALAYSIA.*

*Corresponding Author: ahadi@uthm.edu.my
DOI: https://doi.org/10.30880/ekst.2026.06.01.078

Article Info

Received: 4 January 2026
Accepted: 15 January 2026
Available online: 9 July 2026

Keywords

Wearable Health Monitoring, Nickel Thin Films, PET Flexible Substrate, Strain Sensors, Percolation Threshold

Abstract

The development of wearable health monitoring systems requires high performance materials that can maintain functionality under various physical activities, ranging from sedentary movement to a high intensity exercise. Hence, a material that is both electrically conductive and flexible is beneficial for enhancing the strain sensor's features. Nickel (Ni) is known for its good mechanical properties such as good electrical conductivity, durability and corrosion resistance. Meanwhile, Polyethylene terephthalate (PET) is flexible and also transparent. Both of these are considered good materials to make strain sensors. In this study, Ni thin films were deposited onto the PET substrates using DC magnetron sputtering with deposition time ranging from 6 to 36 minutes at a fixed sputtering current of 60mA. The samples were then characterized through Scanning Electron Microscopy (SEM), Atomic Force Microscopy (AFM), Spectroscopic Ellipsometry, UV-Vis-NIR spectroscopy, and four-point probe to analyse the structural, morphological, optical, and electrical properties of the thin film. Volmer Weber island growth structure can be seen during the morphological analysis. It shows where the isolated nickel islands phase starts to go through the transition phase from the initial nucleation and gradually coalesces with other neighbouring islands as the sputtering time increases.

1. Introduction

The number of wearable health devices has increased since the outbreak of COVID-19 that began in Wuhan, China. Since the virus has a high transmission rate, it rapidly spread and gradually unfolded in the human population. [1]. Wearable devices provide continuous monitoring with minimal user involvement and it is a device that can be use in all work settings. For example, it can track blood pressure, heart rate and temperature without needing to go to the hospital. This invention is useful to humans because it can collect real-time data [2] and give accurate health information and instantly view the results through phone or smartwatches.

Although all these sensors help to monitor internal physiological conditions, it also needs a system that can track physical movement and mechanical changes in the body. For example, strain sensors, where it can detect mechanical deformations, such as body movement or muscle strain, which makes them crucial for applications in motion tracking [3]. Measuring the strength of strain sensors and observing the performance of it is highly dependent on the materials that are being used. Material like Silver has the highest electrical conductivity of all metals and is very sensitive and responsive in sensor systems. It is quite costly, and prone to forming sulfide and chloride films when exposed to some environments, which can degrade its performance with time. Gold offers better chemical stability and corrosion resistance, which makes it suitable for long-term use in corrosive

environments. Meanwhile, in a low temperature surroundings, Nickel (Ni) thin film is more preferred in sensing material. [4]. Other characteristics is Ni has a rapid thermal response and a high sensitivity of resistance to temperature changes. Furthermore, due to the development structure of dense oxide layer on the surface, Ni shows good results of resistance to corrosion and oxidation. [5].

The substrate will act as the base layer in thin film deposition, and its properties can influence the outcome of the film. Polyethylene Terephthalate (PET) emerged as an alternative substrate since it offers greater flexibility, lower cost, and allows for measure and more accurate patterning, especially for applications that needs lightweight and bendable components [6]. Hence, it can be said that PET is much more suitable substrate for deposition of nickel thin film due to its flexibility especially for strain sensor. There are lots of benefits by using Nickel thin films in strain sensor. As the studies of this material for wearable health monitoring system is still on the surface. This study will provide more reasons about Nickel thin films where it offers potential advantages in the form of electrical conductivity and flexibility. In which both are crucial for the device to work and send signals for a real time data.

2. Methods and Materials

2.1 Substrate Preparation

Polyethylene Terephthalate (PET) substrates were prepared in two different sizes, that is, 1 cm × 1 cm and 3 cm × 3 cm, using a cutter. A total of 6 samples were prepared for the experiment, consisting of two different sizes for each deposition condition. The substrates were placed in a beaker for the cleaning process to be done. The cleaning process was performed using a Decon 90 solution to remove any contamination and residues on the surface of the PET substrates. The cleaning solution was prepared by mixing and diluting Decon 90 with tap water with the ratio of 1:10 (one part Decon 90 and ten parts water) and then it was poured in the beaker where the PET substrates were. The handling of Decon 90 was done with the necessary personal protective equipment such as gloves and a face mask due to its chemical nature. After cleaning, the substrates were thoroughly rinsed under running tap water to eliminate the excess solution. The PET substrates were then dried using an air blower to provide a smooth and clean surface before deposition. Subsequently, the substrates were placed in separate petri dishes according to their deposition time, with each petri dish having 2 different sizes of samples and stored in a dry cabinet for 24 hours before the sputtering process began the next day.

2.2 Deposition of Nickel Thin Films

The nickel thin films were deposited on the prepared Polyethylene Terephthalate (PET) substrates using a Quorum Q300TD DC magnetron sputter coater that worked according to the principle of Physical Vapour Deposition (PVD). The cleaned PET substrates were then firmly attached to the sputtering stage using Kapton tape before the deposition process began. The reason for choosing Kapton tape was due to the thermal stability and non-adhesive behaviour, which made the samples to be in a stable position during the exposure to the bombardment of the plasma. Hence, the samples could be easily removed after deposition without leaving any mechanical damage or residual contamination to it.

A turbomolecular vacuum pump was used to evacuate the sputtering chamber to eliminate residual gases and contaminants. The chamber was initially pumped down to a base pressure of approximately 10^{-4} mbar to ensure a clean deposition environment. During deposition, the working pressure was stabilized at approximately 10^{-2} mbar after the introduction of sputtering gas, which is required to sustain a stable plasma for the sputtering process. After completion of the deposition, the chamber was gradually vented back to atmospheric pressure ($\sim 10^{3}$ mbar) to allow safe removal of the samples.

The deposition process involved the ejection of nickel atoms by the high purity nickel target through intense ion bombardment and then deposited onto the PET substrates. All depositions were done with a constant sputtering current of 60 mA to maintain constant plasma conditions. Six samples were made, each having two sizes of substrates of 1 cm × 1 cm and 3 cm × 3 cm. The deposition duration was varied at 6, 12, 18, 24, 30, and 36 minutes to examine how the duration of sputtering affects the film thickness, morphology and functional characteristics. After completing every deposition cycle, the chamber was gradually vented to atmospheric pressure before the samples were removed. The deposited nickel thin films, as shown in Fig. 1, exhibited uniform surface coverage without any visible signs of thermal deformation, melting, or substrate damage to the PET. This observation indicates that the selected sputtering parameters provided sufficient energy for film growth while maintaining thermal compatibility with the flexible polymer substrate.

Excessive heat may lead to substrate deformation, increased internal stress, or poor film adhesion. However, the deposited nickel films exhibited uniform surface coverage without any visible thermal damage to the PET substrate, indicating that thermal effects were adequately controlled under the selected deposition parameters.

Enhanced Knowledge in Sciences and Technology Vol. 6 No. 1 (2026) 698-708

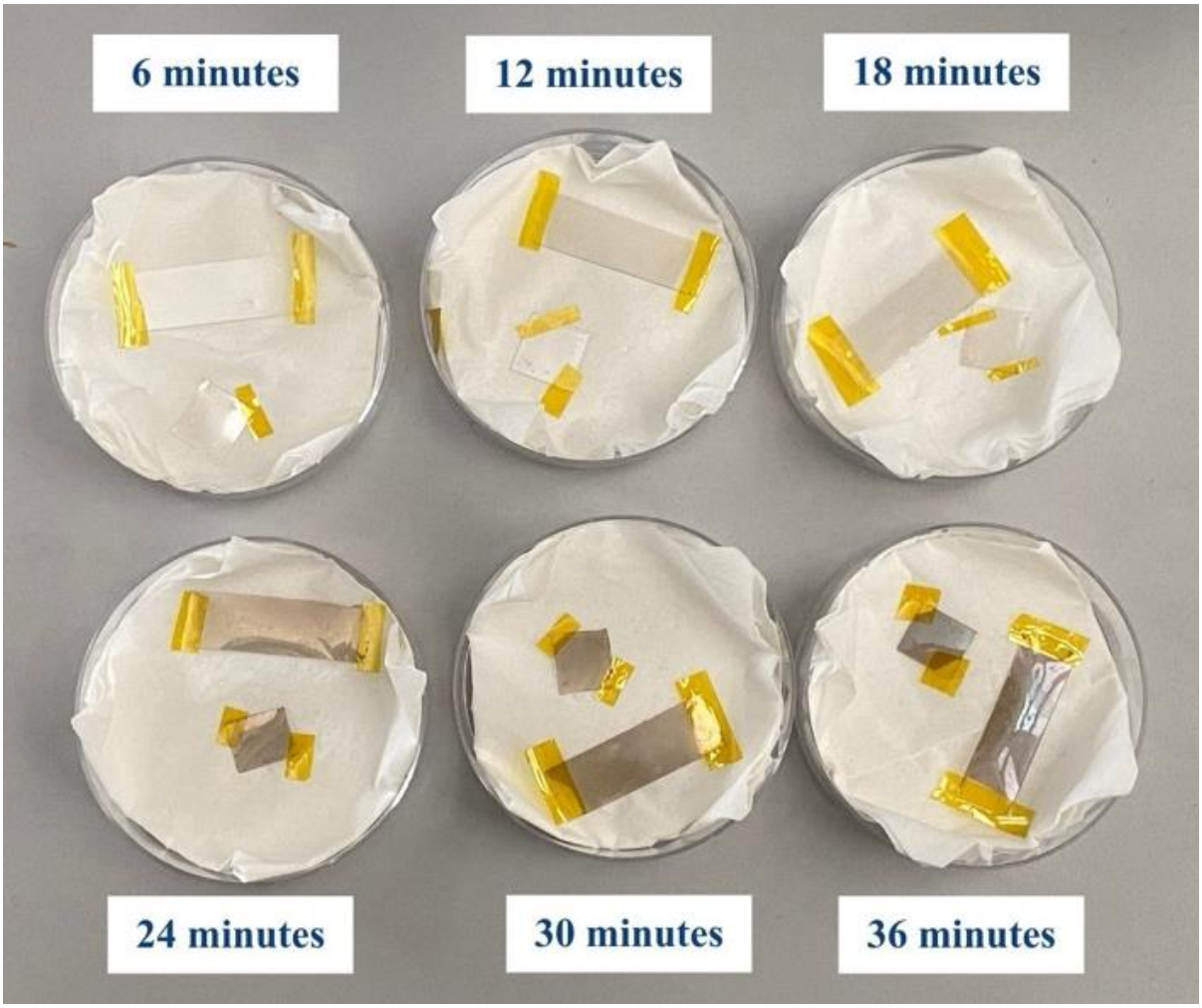

Fig. 1 Samples for Each Deposition Time After Sputtering Process

2.3 Characterization Techniques

Several characterization techniques are used to observe the characterization of the nickel thin film such as Atomic Force Microscopy (AFM), Scanning Electron Microscopy (SEM), Ellipsometry, 4-Point Probe, and UV-Vis-NIR Spectrophotometer. These techniques are used to analyse the topography and roughness using AFM, morphological structure for SEM, Thickness using Ellipsometry, Electrical Characterization using 4-Point probe and the optical transmittance using UV-Vis-NIR Spectrophotometer.

2.3.1 The Film Thickness Measurement using Ellipsometry

The thin films of nickel deposited on PET substrates were measured in terms of optical properties and thickness using a SEMILAB SE-2000 Spectroscopic Ellipsometer fitted with a Quartz Crystal Microbalance (QCM). The Spectroscopic Ellipsometer Analyzer (SEA), version 1.6.5, was used to analyse and obtain the data.

The measurements were made using an ellipsometer with a constant incident angle of 75° and the parameters of the ellipsometer Δ (delta) and Ψ (psi) were measured within the wavelength range 300.2 to 799.98 nm. The regression fitting of the experimental data was performed by the LevenbergMarquardt Algorithm (LMA) and the angular aperture was 0°, which is based on the EllipsoReflectance optical model.

For data interpretation, an optical multilayer model consisting of a thin film layer on a PET substrate was employed. Nickel monosilicide (NiSi) was selected as the reference material for the film phase, while PET was used as the substrate layer. Optical constants at 632.8 nm were set as n = 3.1316 and k = 1.8922 of NiSi, and n = 1.4747 and k = 0 for PET. The NiSi thin film dispersion behaviour was modelled by applying a combination of Drude, Lorentz and Sellmeier dispersion models to get both the free electron and bound electron contributions to the dispersion behaviour.

The reference material was NiSi rather than pure nickel because it would give a better fit to the measured ellipsometric data. This will enhance the stability of the regression process and improve the consistency between the experimental outcomes and the optical model, which can lead to more accurate thickness and optical parameter extraction.

2.3.2 Optical Transmittance using UV-Vis-NIR

Optical transmittance characteristics of nickel thin films deposited on PET substrates were determined by a Shimadzu UV-3600Plus UV -Vis-NIR spectrophotometer in normal transmittance mode and with a double beam configuration. The measurements were conducted in a range of wavelengths of 300-1100 nm to encompass the ultraviolet, visible and near-infrared. The slit width was set to 1.0 nm and a sampling interval of 2.0 nm so that there was sufficient spectral resolution.

The samples size of 1 cm x 3 cm were placed in the sample holder in an upright position to enable the incident light to pass through the film perpendicular to the surface. To correct the baseline and normalize the transmittance spectra, a bare PET substrate was used to subtract substrate based optical contributions.

The obtained transmittance data were recorded and processed using the Shimadzu analysis software to produce transmittance (T) versus wavelength spectra. Optical behaviour of the films was determined by observing the alterations on optical transmittance and changes on the absorption edge with respect to deposition time. These changes give an understanding of the development of thickness, growth in light absorption and the transition from discontinuous to semi continuous metallic film structures.

2.3.3 Morphological Analysis Observation using Scanning Electron Microscopy (SEM)

Surface morphology of nickel thin films deposited on PET substrates was examined using a COXEM EM-30AX Scanning Electron Microscope (SEM) equipped with a DVA-T56 detector. SEM analysis was performed to investigate the surface features, film uniformity, and growth behaviour of the nickel thin films as a function of deposition time. The samples were examined without any conductive coating, as the metallic nature of nickel provided sufficient surface conductivity for electron imaging.

Before imaging, acetone was used to clean aluminium SEM stubs to remove surface contaminants, and to promote good adhesion. The nickel-coated PET samples were then mounted onto the cleaned stubs using conductive adhesive tape to provide stable positioning during observation. Careful handling was applied throughout the preparation process to minimize contamination and surface artifacts.

All observations made by SEM were done under the same operating conditions to allow a comparative analysis of samples. The accelerating voltage was set to 20kV, the working distance was set to 11.2 mm, and the spot size was set to 10. To clearly show the nanoscale features on the film surface, the surface morphology was imaged at 5000× magnification and the sample characterization through SEM was only done using samples with the size of 1 cm x 1 cm.

2.3.4 Surface Topology using Atomic Force Microscopy

A Park Systems XE-100 Atomic Force Microscope (AFM) was used to characterize the topography of a nickel thin film deposited on PET substrates in terms of its three-dimensional surface topography and nanoscale roughness. The measurements were all taken in true non-contact mode to avoid physical contact between the probe tip and the sample surface. This mode was chosen so as not to damage the fragile nickel islands and the soft PET substrate and therefore maintain the original morphology of the surface during scanning.

To analyse using AFM, all samples were cut into 1 cm × 1 cm size so that they fit the AFM sample stage and that they could be placed stably on the stage during the analysis. The samples were attached to the AFM magnetic puck with the use of the double-sided adhesive tape to reduce the vibration and interlateral movement during scanning.

A scan size of 5 μm × 5 μm was going to be used to capture the global surface properties and to capture the morphological change between isolated nickel islands to a semi-continuous network with longer deposition time. To capture fine surface features, the scans were done at 0.5 to 1 Hz scan rate and 256 × 256 pixels. The parameters of surface roughness were measured on the AFM data and correlated the morphological evolution with optical and electrical properties.

2.3.5 Film Conductivity Analysis using 4-Point Probe

A four-point probe system based on a linear system with Keithley 2450 SourceMeter (SMU) was used to assess the electrical characteristics of nickel thin films deposited on PET substrates. A four-point probe set-up, where the tungsten tips are positioned in a linear manner, was used to reduce the effects of contact resistance. The applied current was sourced on the two outer probes and the voltage drop across the film was measured across the two inner ones. Thickness values required for four-point probe resistivity calculations were obtained from spectroscopic ellipsometry, with film thickness ranging from approximately 7.88 nm to 27.02 nm.

In current sweep mode, electrical measurements were done to determine current voltage (I-V) characteristics and ohmic behaviour of the nickel thin films. The current applied was changing between 0 to 10 mA and voltage compliance was set to 5.0 V, this is to avoid electrical damages on the thin films. The measurements were all conducted on the samples of the size 1 cm × 3 cm and positioned on a sample stage that is insulated.

Enhanced Knowledge in Sciences and Technology Vol. 6 No. 1 (2026) 698-708

The resistivity of the samples was determined using the measured sheet resistance, which was obtained by film thickness values obtained in spectroscopic ellipsometry. The electrical data were examined to observe the change in the insulating behaviour in the early nucleation stage to metallic percolation with different deposition time.

3. Results and Discussion

3.1 Optical Properties and Thickness Evolution of Sputtered Nickel Films

Spectroscopic ellipsometry was used to measure the thickness of the sputtered nickel thin films by measuring the ellipsometric parameters Psi and Delta shown in Fig 2 and Fig 3, which are the ratio of amplitude and the phase difference between the p-polarized and the s-polarized reflected light. These parameters are extremely sensitive to the thickness of the film, where any variation in thickness changes optical path length and conditions of interference in the thin film.

There were systematic variations of Ψ and Δ with deposition time that allowed effective extraction of thickness by optical modelling. Based on Table 1, the thickness values extracted are increasing non-linearly at a rate of around 7.88 nm at 6 minutes to 24.2 nm at 24 minutes, followed by a slower increase to approximately 27.0 nm at 36 minutes. The rapid thickness increase at early deposition stages is attributed to island-type nucleation and porous film formation, while the reduced growth rate beyond 24 minutes is associated with void filling and film densification after the percolation threshold [7].

These results indicate a transition from discontinuous island growth to a denser quasi-continuous nickel layer, consistent with the Volmer–Weber growth mode observed in the morphological analysis [8].

Table 1 Variation of nickel thin film thickness and growth regime with sputtering duration

Sputtering Time (min)	Measured Thickness (nm)	RMSE (Fit Quality)	Extinction Coeff. (k)	Growth Phase
6	7.88	0.71	1.89	Nucleation (Island Formation)
12	14.35	0.73	0.88	Nucleation (Island Formation)
18	22.34	0.25	0.72	Early Coalescence
24	24.20	21.09	2.98	Percolation Threshold (Conductive Path)
30	25.52	0.97	1.09	Continuous Film
36	27.02	0.93	0.86	Continuous Bulk-like Film

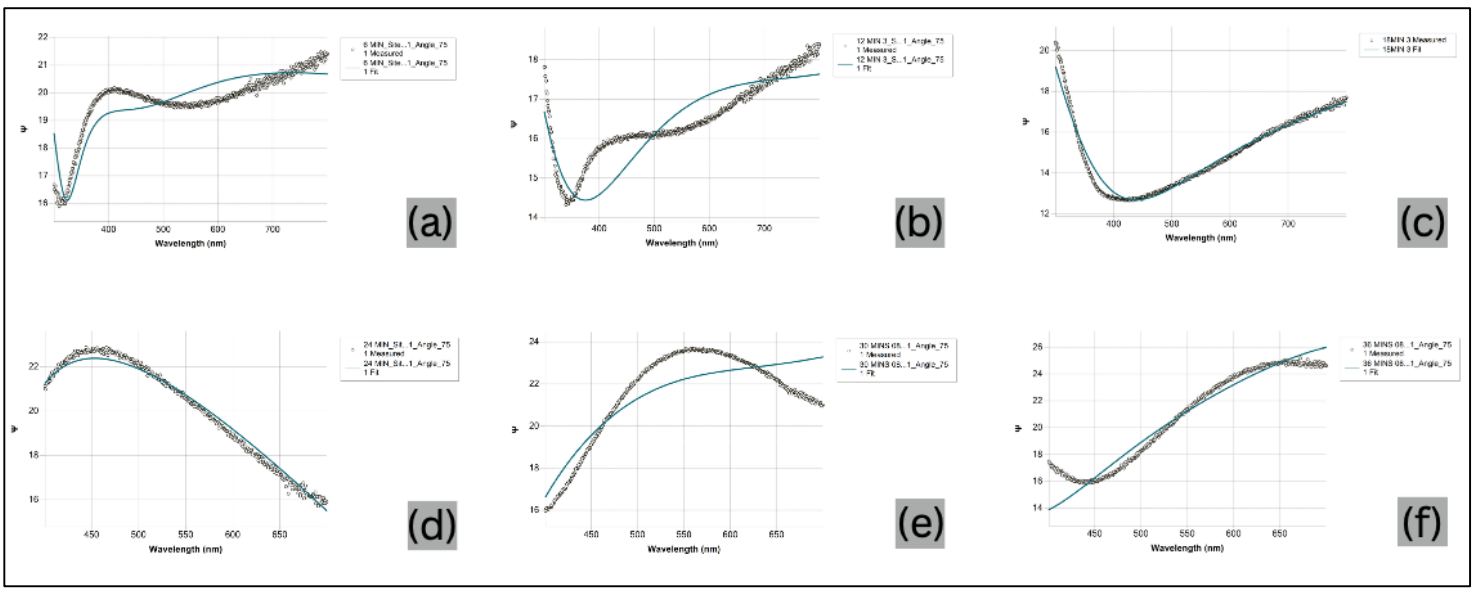

Fig. 2 Regression Graph of Psi at (a) 6 minutes; (b) 12 minutes; (c) 18 minutes; (d) 24 minutes; (e) 30 minutes; (f) 36-minute deposition time

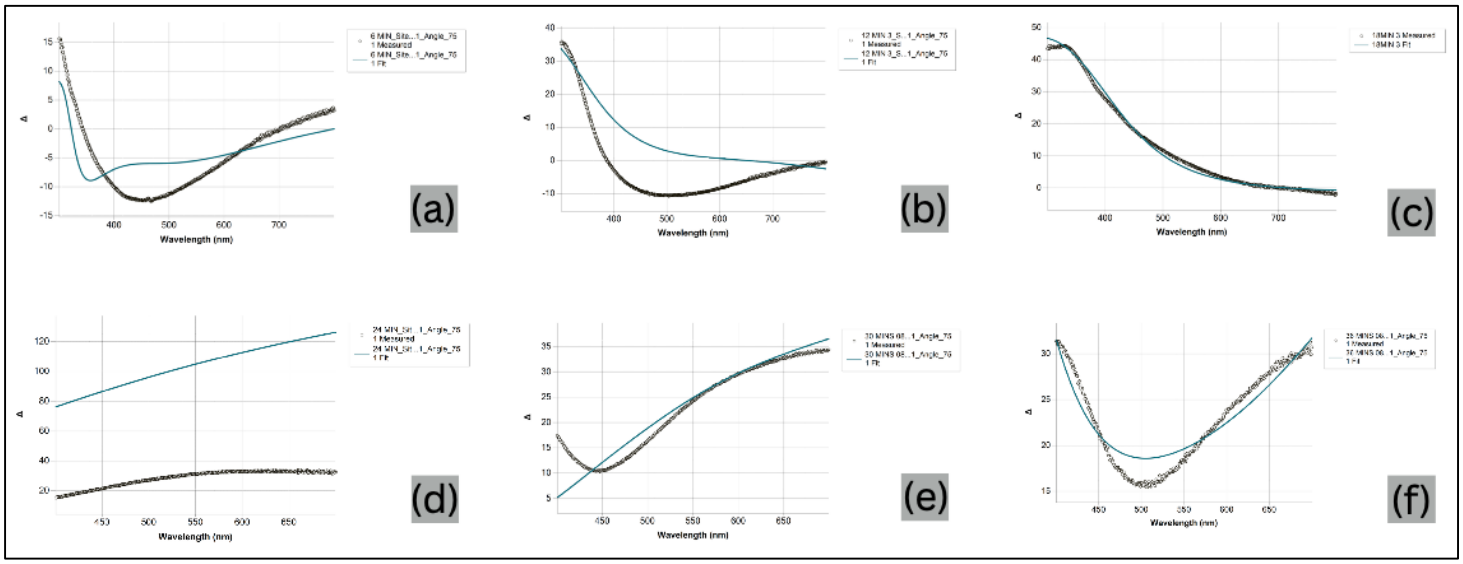

Fig. 3 Regression Graph of Delta at (a) 6 minutes; (b) 12 minutes; (c) 18 minutes; (d) 24 minutes; (e) 30 minutes; (f) 36-minute deposition time

3.2 Optical Transmittance Evolution and Transparency-Conductivity Trade-off

The UV-Vis-NIR spectroscopy shows a strong dependence of optical transmittance on film morphology. Films deposited for 6 minutes are highly transparent (>80%) based on Fig 4, because the discontinuous island structure allows transmission of light through exposed PET regions. With increased deposition time to 12 and 18 minutes, transmittance is decreased as a result of more surface coverage and light absorption by the growing nickel clusters [9].

A pronounced minimum in transmittance is observed at 24 minutes, corresponding to the percolation threshold. The extremely disordered surface at this stage causes a high degree of light scattering, which causes a lower optical transparency [10]. Interestingly, there is a partial recovery in the transmittance at 30 minutes despite the addition in thickness. AFM analysis confirms that this behaviour is due to surface planarization, which reduces diffuse scattering. At 36 minutes, the film exhibits bulk-like metallic behaviour with consistently low transmittance (<50%).

These results emphasize a trade-off of crucial significance between optical transparency and electrical conductivity, which is determined mainly by nanoscale surface morphology, and not necessarily by thickness.

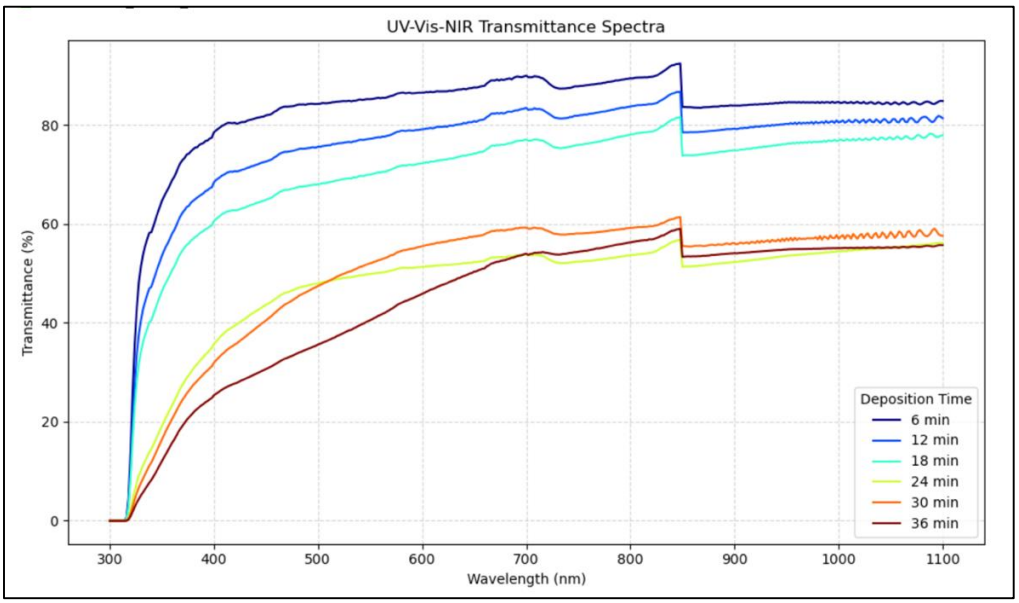

Fig. 4 Spectral Data of UV-VIS-NIR Spectrophotometer for samples from 6 to 36 minutes

Enhanced Knowledge in Sciences and Technology Vol. 6 No. 1 (2026) 698-708

3.3 Morphological Characterization of Nickel Thin Film of SEM & EDS Analysis

The structure of the nickel thin films that were sputtered on PET substrates was examined with deposition time ranging from 6 to 36 minutes. SEM and EDS analysis show that there is a time-dependent transition in film growth behaviour. Nickel is observed to nucleate at short deposition durations of 6-12 minutes as isolated islands on PET surface and supported by the low nickel weight percentages of less than 3 wt% based on Fig 5 and discontinuous surface morphology. This can be related to the characteristic of VolmerWeber island growth that is due to the weak interfacial adhesion between metallic films and polymer substrates [11].

As the deposition time is increased to 18 minutes, the coalescence of the island is noticed with the moderate growth in nickel composition. The fact that the nickel content has significantly increased to (~15.7 wt) after 24 minutes shows that the percolation threshold has been formed, as the neighboring nickel islands have started to connect and create continuous conductive pathways across the substrate [12]. Additional sputtering at 30- and 36-minutes leads to more advanced and densified nickel films as seen by stabilized nickel compositions over 15 wt%. While individual grain boundaries are not distinctly resolved at the applied SEM magnification in Fig 6, the combined SEM contrast and compositional tendencies confirm a clear transition from isolated island growth toward a quasi-continuous metallic film.

Altogether, the morphological evolution in Table 2 shows that the process of transition between the initial-stage nucleation and the films involving interconnections and thickening is due to deposition-time-dependent. This is essential in controlling the electrical transport properties of the nickel thin films, especially in determining the ideal growth regime of the latter in flexible electronic and strain sensing applications.

Table 2 Comparison of SEM Morphology and EDS Composition for All Deposition Times

Deposition Time	SEM Morphology (5kx)	Ni (wt%)	C (wt%)	O (wt%)	Yb (wt%)	Microstructure Stage
6 min	No grains, island growth, tiny bright spots, low contrast, dust contamination	1.12	68.54	30.34	-	Initial nucleation
12 min	Small, grains begin forming, slightly higher density, scratches visible	2.78	61.90	35.32	-	Early nucleation turns to partial coalescence
18 min	Grain visibility still low, larger dark/bright patches, noticeable scratches	3.12	59.02	37.85	-	Late nucleation / early growth
24 min	Smoother surface, very low contrast, large scratches and contamination spots	15.68	36.27	38.83	9.21	Transition to continuous film
30 min	Dense and uniform, smoother than earlier, dark patches exist	15.13	38.19	40.10	6.58	Advanced coalescence
36 min	Most uniform, scratches prominent, low contrast, slight thickness variation	18.31	31.82	41.07	8.80	Near-continuous film

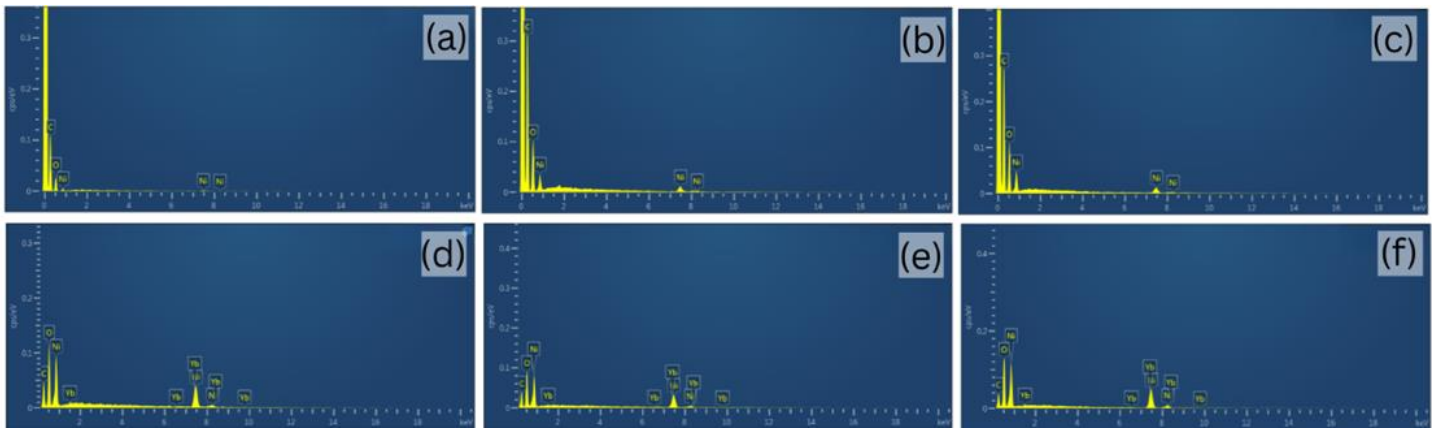

Fig. 5 EDS spectrum Analysis of Ni thin film on PET for (a) 6 minutes; (b) 12 minutes; (c) 18 minutes; (d) 24 minutes; (e) 30 minutes; (f) 36 minutes, showing elemental composition (C,O, Ni)

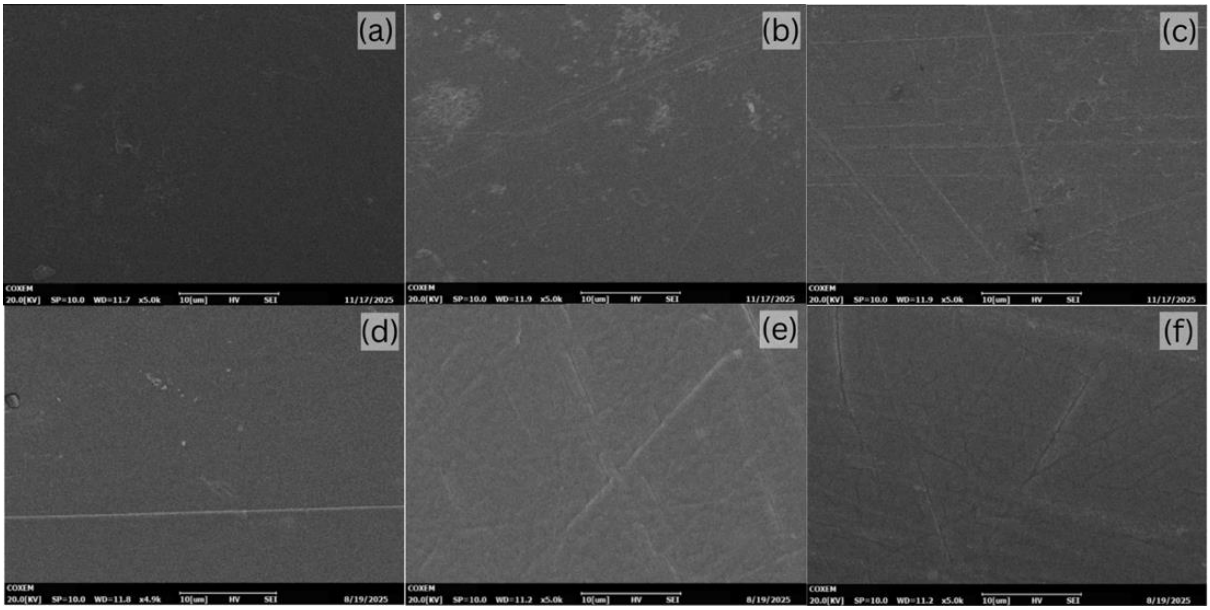

Fig. 6 SEM Image Showing Grain Features of Ni Thin Film on PET Observed at 5kx Magnification Different Deposition Time of (a) 6 minutes; (b) 12 minutes; (c) 18 minutes; (d) 24 minutes; (e) 30 minutes; (f) 36 minutes

3.4 Nanoscale Surface Topography and Morphological Evolution of Nickel Thin Films

The topography and roughness changes of the surface of sputtered nickel thin films were evaluate using atomic force microscopy (AFM) at different deposition time ranging from 6 to 36 minutes. The root-mean-square (RMS) roughness shows a non-monotonic trend in Fig 8, which is an indication of the change of growth mechanism when forming the film. The films exhibit relatively low-surface roughness of about 7.5 nm at early times of deposition (6 minutes) which is in line with isolated island nucleation and low surface coverage as can be seen in Fig 7.

The roughness RMS of the deposition from Table 3 increases with the deposition time to a peak of about 29.5 nm at 24 minutes, which is the percolation threshold. This roughness peak is explained by active coalescence of islands, height variation and surface disorder in the process of creating interconnected conductive pathways [13]. The pronounced surface roughness at this stage contributes to enhanced optical scattering and influences electrical transport behaviour.

As additional deposition occurs at 30 and 36 minutes, the RMS roughness substantially decreases, which is an indication that surfaces are being smoothed and films densified by filling in the voids and subsequent growth of the lateral grains [14]. This decrease in roughness correlates with the stabilization of electrical resistivity and the partial recovery of optical transmittance, which proves that surface morphology is an essential factor in determining the multifunctionality of the sputtered nickel thin films.

Enhanced Knowledge in Sciences and Technology Vol. 6 No. 1 (2026) 698-708

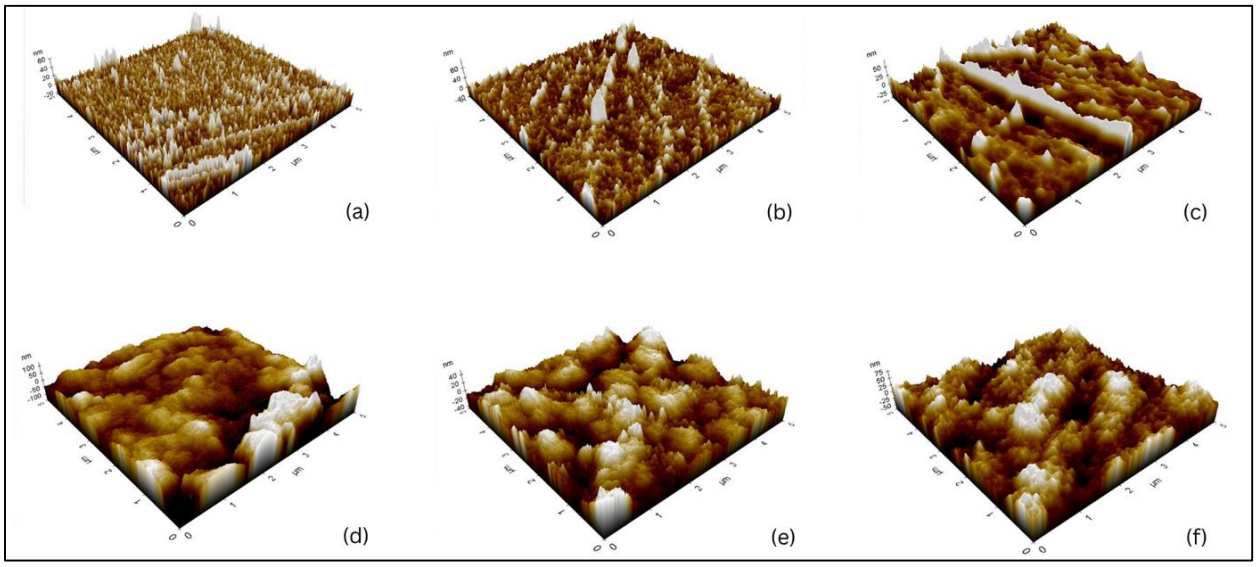

Fig. 7 3D Surface Topography of Nickel Thin Film Exhibiting Isolated Island Morphology for samples of (a) 6 minutes; (b) 12 minutes; (c) 18 minutes; (d) 24 minutes; (e) 30 minutes; (f) 36 minutes

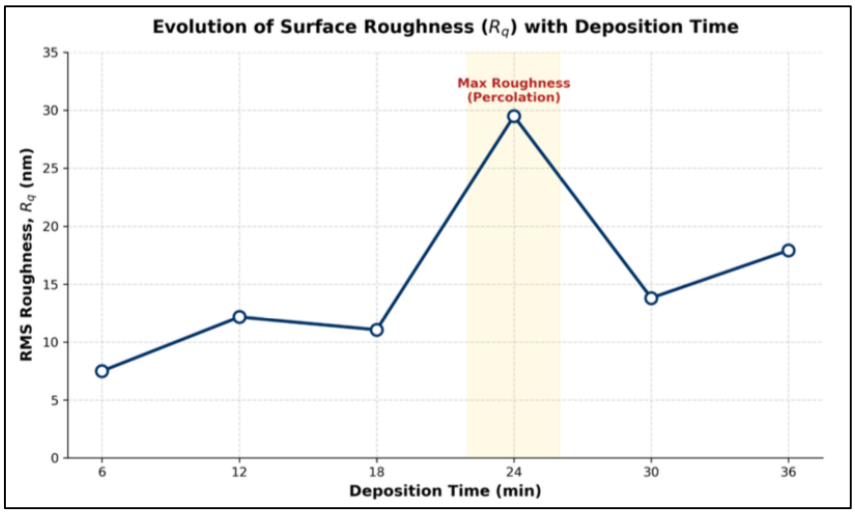

Fig. 8 The surface roughness $\boldsymbol{R_q}$ of Nickel Thin Films at Different Deposition Time

Table 3 Surface roughness parameters (Ra, Rq, and Rz) obtained from AFM analysis

Deposition Time (min)	Thickness (nm)	Ra (nm)	Rq (nm)	Rz (nm)
6	7.88	5.68	7.50	82.92
12	14.35	8.46	12.16	153.68
18	22.34	7.88	11.06	108.56
24	24.20	21.93	29.49	261.66
30	25.52	11.03	13.80	97.37
36	27.02	14.02	17.91	143.58

3.5 Electrical Characterization and Microstructural Evolution of Nickel Thin Films

A four-point probe electrical characterization indicates a strong correlation between resistivity and the film thickness. At early deposition times of 6-18 minutes, the films exhibit high resistivity because of isolated nickel islands and electron tunnelling-driven transport [15]. There is an abrupt decrease can be observed in resistivity between 18 and 24 minutes, decreasing from ~162 Ω·cm to ~14.7 Ω·cm, see Fig. 9. This sharp transition marks the percolation threshold, where continuous conductive pathways are formed across the substrate.

For thicker films deposited at 30 and 36 minutes, the resistivity stabilizes in the range of 14–17 Ω·cm in Table 4. These slight differences are attributed to the effect of grain boundary and surface scattering effects, which are common in thin metallic films [16]. Electrical property stabilization proves the development of an extensive conductive structure that can be used in strain-sensing.

Table 4 Average Resistivity for Different Sputtering Time and Thickness

Sputtering Time (mins)	Thickness (nm)	Average Resistivity (Ω cm)
6	7.88	80.39
12	14.35	162.10
18	22.34	162.05
24	24.20	14.66
30	25.52	14.7
36	27.02	17.72

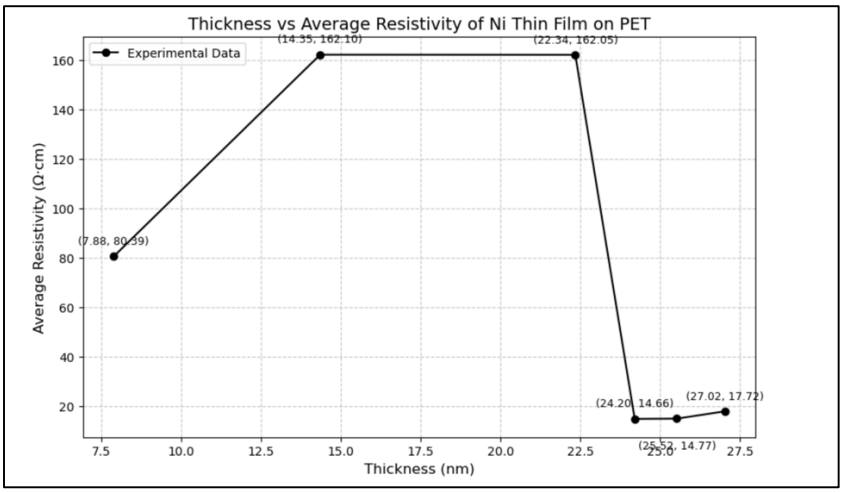

Fig. 9 Graph for Thickness vs Average Resistivity of Ni thin film on PET

4. Conclusion

The properties and growth behaviour of the sputtered nickel thin films deposited on flexible PET substrates were systematically studied with respect to deposition time in this study. The morphological analysis verifies that with time there is a change of isolated island nucleation to a more continuous quasi-film structure, as would be predicted by the Volmer Weber growth mode. This development is facilitated by compositional, thickness, optical and electrical characterizations.

Spectroscopic ellipsometry shows a non-linear increase of the thickness with the deposition time ranging from approximately 7.88 nm at 6 minutes to a stabilized thickness of about 27.0 nm at 36 minutes, which indicates the porous island growth and the densification of the film after the percolation threshold. The morphology-driven optical response is demonstrated by UV- Vis transmittance measurements, where increased surface roughness and scattering near the percolation regime led to reduce transparency. Electrical characterization also confirms a sharp percolation transition between 18 and 24 minutes, where resistivity significantly decreases followed by stabilization at a higher deposition time.

Overall, the results demonstrate that deposition time plays a critical role in governing the structural, optical, and electrical performance of sputtered nickel thin films. The identification of the percolation threshold and stabilized conductive regime highlights the suitability of these films for flexible electronic and strain-sensing applications.

Acknowledgement

This author(s) appreciates the Government of Malaysia and Universiti Tun Hussein Onn Malaysia for funding this research project through the UTHM TIER1 Grant (Q417).

Conflict of Interest

Authors declare that there is no conflict of interests regarding the publication of the paper.

Author Contribution

The authors confirm contribution to the paper as follows: ***study conception and design, data collection, analysis and interpretation of results, draft manuscript preparation:*** *Nur Khairunnisa Amrang, Ahmad Hadi Ali. All authors reviewed the results and approved the final version of the manuscript.*

References

[1] Liu, Y. C., Kuo, R. L., & Shih, S. R. (2020). COVID-19: The first documented coronavirus pandemic in history. In Biomedical Journal (Vol. 43, Number 4, pp. 328–333). Elsevier B.V. https://doi.org/10.1016/j.bj.2020.04.007

[2] Channa, A., Popescu, N., Skibinska, J., & Burget, R. (2021). The rise of wearable devices during the COVID-19 pandemic: A systematic review. In Sensors (Vol. 21, Number 17). MDPI AG. https://doi.org/10.3390/s21175787

[3] Farooq, M., & Sazonov, E. (2015). Strain sensors in wearable devices. In *Smart Sensors, Measurement and Instrumentation* (Vol. 15, pp. 221–239). Springer International Publishing. https://doi.org/10.1007/978-3-319-18191-2_9

[4] Cui, J., Liu, H., Li, X., Jiang, S., Zhang, B., Song, Y., & Zhang, W. (2020). Fabrication and characterization of nickel thin film as resistance temperature detector. Vacuum, 176. https://doi.org/10.1016/j.vacuum.2020.109288

[5] Kawashima, A., Habazaki, H., & Hashimoto, K. (2001). Highly corrosion-resistant Ni-based bulk amorphous alloys. In Materials Science and Engineering A304 (Vol. 306).

[6] Liang, C. H., & Qi, X. (2013). Indium-tin-oxide thin films deposited on polyethylene-terephthalate substrates by substrate-biased RF magnetron sputtering. Surface and Coatings Technology, 231, 205–208. https://doi.org/10.1016/j.surfcoat.2012.06.068

[7] Hedl, E., Bregović, V. B., Rakić, I. Š., Mandić, Š., Samec, Ž., Bergmann, A., & Sancho-Parramon, J. (2023). Optical properties of annealed nearly percolated Au thin films. *Optical Materials*, *135*. https://doi.org/10.1016/j.optmat.2022.113237

[8] Liu, P., Shi, Z., Teng, D., Liu, F., Cao, Y., Lin, Y., Yang, Z., Yang, A., Zheng, Y., & Chen, L. (2023). Optical Characteristics of Silver Thin Films from Island to Percolation in the Ultra-Wide Infrared Spectral Range. *Coatings*, *13*(11). https://doi.org/10.3390/coatings13111910

[9] Chen, W. F., Koshy, P., & Sorrell, C. C. (2016). Effects of film topology and contamination as a function of thickness on the photo-induced hydrophilicity of transparent TiO2 thin films deposited on glass substrates by spin coating. *Journal of Materials Science*, *51*(5), 2465–2480. https://doi.org/10.1007/s10853-015-9559-y

[10] Axelevitch, A., Gorenstein, B., & Golan, G. (2012). Investigation of Optical Transmission in Thin Metal Films. *Physics Procedia*, *32*, 1–13. https://doi.org/10.1016/j.phpro.2012.03.510

[11] Magnfält, Daniel. (2014). Fundamental Processes in Thin Film Growth : The Origin of Compressive Stress and the Dynamics of the Early Growth Stages. Linkopings Universitet.

[12] Cama, E. S., Pasini, M., Giovanella, U., & Galeotti, F. (2025). Crack-Templated Patterns in Thin Films: Fabrication Techniques, Characterization, and Emerging Applications. In *Coatings* (Vol. 15, Issue 2). Multidisciplinary Digital Publishing Institute (MDPI). https://doi.org/10.3390/coatings15020189

[13] Pahwa, N., & Singh, A. R. (2025). "Structural, Optical and AFM based PSD surface roughness studies of cadmium telluride thin films of nanometer thickness range." *Results in Surfaces and Interfaces*, *21*. https://doi.org/10.1016/j.rsurfi.2025.100655

[14] Zouari, M., Stanciu, S. G., Jakes, J., Marrot, L., Fiorentis, E., Stanciu, G. A., & DeVallance, D. B. (2023). Investigations on the topography and micro-mechanical properties of polyvinyl alcohol thin-film composites reinforced with hardwood biocarbon particles. *Journal of Materials Research and Technology*, *27*, 5533–5540. https://doi.org/10.1016/j.jmrt.2023.10.217

[15] Karakuş, E., Mehmet Koç, M., & Coşkun, B. (2024). A Brief Overview for Fundamental Electrical Characterization Techniques for Thin Films and Nanostructures. In *Journal of Materials and Electronic Devices* (Vol. 1).

[16] Likius, D. S., Nagai, H., Aoyama, S., Mochizuki, C., Hara, H., Baba, N., & Sato, M. (2012). Percolation threshold for electrical resistivity of Ag-nanoparticle/titania composite thin films fabricated using molecular precursor method. *Journal of Materials Science*, *47*(8), 3890–3899. https://doi.org/10.1007/s10853-011-6245-6